

Superbases in Confined Space: Control of the Basicity and Reactivity of the Proton Transfer

Bastien Chatelet,[†] Heinz Gornitzka,^{‡,§} Véronique Dufaud,^{||} Erwann Jeanneau,[⊥] Jean-Pierre Dutasta,^{*,†} and Alexandre Martinez^{*,†}

[†]Laboratoire de Chimie, École Normale Supérieure de Lyon, CNRS, UCBL, 46 Allée d'Italie, F-69364 Lyon, France

[‡]Laboratoire de Chimie de Coordination du CNRS, 205 Route de Narbonne, BP 44099, F-31077 Toulouse Cedex 4, France

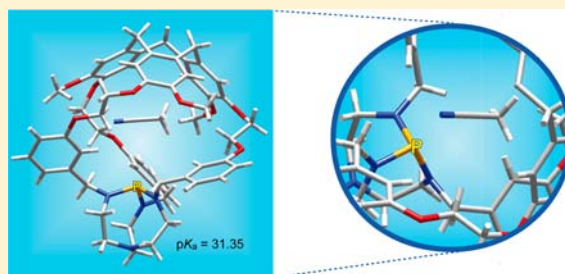
[§]Université de Toulouse, UPS, INPT, F-31077 Toulouse Cedex 4, France

^{||}Laboratoire de Chimie, Catalyse, Polymère, Procédés (C2P2), Université de Lyon, CNRS, Université Claude Bernard Lyon1, CPE Lyon, 43 Boulevard du 11 Novembre 1918, F-69616 Villeurbanne Cedex, France

[⊥]Centre de Diffractométrie Henri Longchambon, Université Claude Bernard Lyon 1, Site CLEA—Bâtiment ISA, 5 Rue de La Doua, F-69100 Villeurbanne, France

Supporting Information

ABSTRACT: Endohedral functionalization of the molecular cavity of host molecules is in high demand in many areas of supramolecular chemistry. When highly reactive species are incarcerated in the confined space of a molecular cavity, deep changes of their chemical properties are expected. Here, we show that the superbasic properties of proazaphosphatranes can be improved in the confined space of the molecular cavity of hemicryptophane hosts. A general and modular procedure is described to prepare supramolecular superbases with various cavity sizes. The rate of proton transfer is strongly dependent on the shape and size of the inner cavity of the designed superbasic structure. Kinetic and thermodynamic data are strongly correlated to the space available around the basic center as revealed by the X-ray molecular structures analyses.

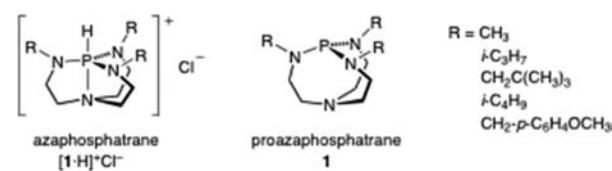


1. INTRODUCTION

The kinetics and thermodynamics of proton transfer in biological systems can be strongly modified by the surrounding medium.^{1–3} Changes in the reactivity in such confined biological entities have driven chemists to try to explain and to mimic them through the design of supramolecular structures.^{4–13} Indeed, the specific size, shape, and chemical environment encountered in a confined nanospace induce a guest molecule to new activities and selectivities by imposing specific orientations and conformations. Therefore, nanosized reaction chambers (i.e., nanoreactors, combining a basic site and a binding pocket) creating a confined and well-defined nanospace around the substrates have been synthesized.^{14–18} For instance, molecular capsules with functionalized inner surfaces are accessible by following sophisticated synthetic approaches.¹⁹ The development of coordination self-assemblies also afforded endofunctionalized noncovalent cage complexes.^{20–24} The endohedral location of basic functional groups, in particular tertiary amines, strongly affects the thermodynamic and kinetic behaviors of the encapsulated function. However, quantitative studies of the effect of encapsulation of tailored highly basic species still remain an unexplored area of research.

The proazaphosphatranes **1**, with the related azaphosphatranes $[I\cdot H]^+Cl^-$ (Chart 1), first synthesized by Verkade et al.,²⁵ are nonionic superbases ($pK_a \approx 32$) now broadly used in

Chart 1. Azaphosphatrane and Proazaphosphatrane Derivatives



organic synthesis as stoichiometric bases and as catalysts.^{26–36} Recently, we reported the synthesis of an engaged proazaphosphatrane superbase in a hemicryptophane-type structure, and we investigated the thermodynamic and kinetic consequences of the encapsulation.³⁷ This study showed that encapsulation does not alter the strong basicity of the proazaphosphatrane but dramatically decreased the rate of proton transfer. Herein, we wish to demonstrate how the size and the shape of the nanospace around this highly reactive center can control the basicity and the rate of the proton transfer. We thus synthesized new engaged proazaphosphatrane superbases, having a molecular cavity with different volumes and shapes, above the reactive center. These tailored-made nanoreactors provide a

Received: September 23, 2013

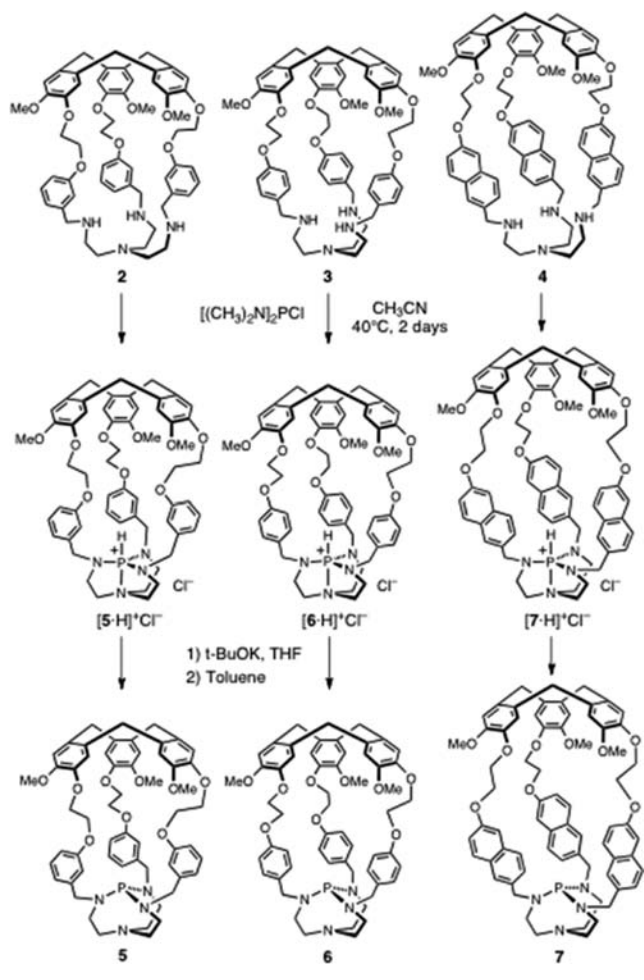
Published: November 14, 2013

unique tool to study how confinement can affect the behavior of an engaged active site. The closed space of the molecular cavity is shown to have a dramatic effect on the rate of the proton transfer and the basicity of the proazaphosphatranes, which can be more than 100 times more basic or 30 times less basic than their model counterparts without cavity. These results are rationalized thanks to the X-ray structure analysis of the molecules, highlighting how the inner space of the host changes the properties of the encapsulated active site.

2. RESULTS AND DISCUSSION

2.1. Synthesis of the Hemicyptophane Superbases and the Model Compounds. We have reported previously a modular synthesis of hemicyptophane hosts, allowing an easy modification of the size and shape of the inner cavity. This provides an unprecedented tool to change the architecture of the supramolecular host and thus to study how the size and shape of the nanospace can affect the proton transfer. The three *tren*-hemicyptophane precursors 2–4 (Scheme 1) were

Scheme 1. Synthesis of the Supramolecular Proazaphosphatrane Superbases

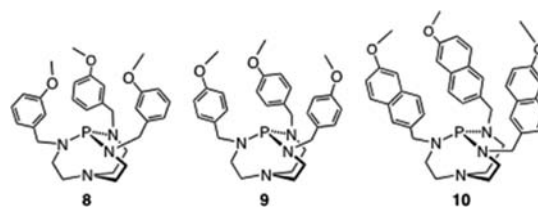


obtained following our previous procedure.³⁸ They display similar functionalities but differ by the size of their cavity. We have already described elsewhere the synthesis of 6 and its conjugate acid $[\text{6-H}]^+\text{Cl}^-$.³⁷ The syntheses of the new phosphatrane–hemicyptophanes $[\text{5-H}]^+\text{Cl}^-$ and $[\text{7-H}]^+\text{Cl}^-$ were performed using similar experimental conditions (Scheme

1): addition of hemicyptophane 2 or 4 to a solution of $[(\text{CH}_3)_2\text{N}]_2\text{P-Cl}$ in acetonitrile afforded the encapsulated azaphosphatrane $[\text{5-H}]^+\text{Cl}^-$ or $[\text{7-H}]^+\text{Cl}^-$ in 32% or 36% yield, respectively.³⁹ They were then deprotonated using potassium *tert*-butoxide in THF followed by extraction with toluene to give the engaged superbases 5 and 7. The weak acids $[\text{5-H}]^+\text{Cl}^-$ and $[\text{7-H}]^+\text{Cl}^-$ displayed a single ^{31}P NMR signal at -32 and -36 ppm in CDCl_3 , respectively, which is significantly highfield shifted of about 20 ppm compared to other azaphosphatranes^{29–36} but consistent with that of $[\text{6-H}]^+\text{Cl}^-$.³⁷ In $\text{THF-}d_8$ compounds 5 and 7 showed a ^{31}P NMR signal at 125 and 118 ppm, respectively, as expected for proazaphosphatrane derivatives.

It has been shown that the basicity of the proazaphosphatranes depends on the nature of the substituents on the nitrogen atoms.^{26–28} Thus, to explore the effects of the environment and of the confinement on the activity of the phosphorus superbases, we synthesized the related model compounds 8–10 (Chart 2) in a three-step sequence starting from tris-(2-aminoethyl)amine and the corresponding aldehyde, according to the procedure already described for 9 (see Supporting Information).

Chart 2. Model Superbases



2.2. Structural Studies. The X-ray structures of hemicyptophanes 5, $[\text{7-H}]^+\text{Cl}^-$, and the model compound $[\text{9-H}]^+\text{Cl}^-$ were obtained, allowing for study of the role of confinement on the superbasic properties of these derivatives. The molecular structure of $[\text{6-H}]^+\text{Cl}^-$ has been described previously and is reported here for the discussion.³⁷ The molecular structures of $[\text{6-H}]^+\text{Cl}^-$, $[\text{7-H}]^+\text{Cl}^-$, and $[\text{9-H}]^+\text{Cl}^-$ clearly show the atrane structure of the phosphorus moiety, which for $[\text{6-H}]^+\text{Cl}^-$ and $[\text{7-H}]^+\text{Cl}^-$ is located inside the molecular cavity of the hemicyptophane host (Figure 1). Surprisingly, proazaphosphatrane 5 cocrystallized with the Verkade's superbase 1 ($\text{R} = \text{CH}_3$) from the acetonitrile solution used for the determination of its $\text{p}K_a$ value. Both substrates lie in the unit cell without interaction, which allows the resolution of the first X-ray structure of an engaged Verkade's superbase. In 5 the reactive lone pair of the phosphorus atom is oriented toward the inner cavity of the hemicyptophane, specifying the endohedral functionalization of the host compound (Figure 1).

The geometric parameters around the phosphorus atoms are reported in Table 1. The equatorial P-N_{eq} bond lengths and the apical P-N_{ap} distance in $[\text{6-H}]^+\text{Cl}^-$, $[\text{7-H}]^+\text{Cl}^-$, and $[\text{9-H}]^+\text{Cl}^-$ are in the range of typical values determined for phosphatrane derivatives.^{25,28–36} In the latter the trigonal bipyramidal geometry around the phosphorus atom is characterized by the sum of the $\text{N}_{\text{eq}}\text{-P-N}_{\text{eq}}$ angles of $358\text{--}359^\circ$ and the average $\text{N}_{\text{eq}}\text{-P-N}_{\text{ap}}$ angle of 86° . More interesting are the shape and the size of the molecular cavity that strongly depends on the aromatic linkers that bind the CTV cap to the phosphatrane unit. To investigate this, we

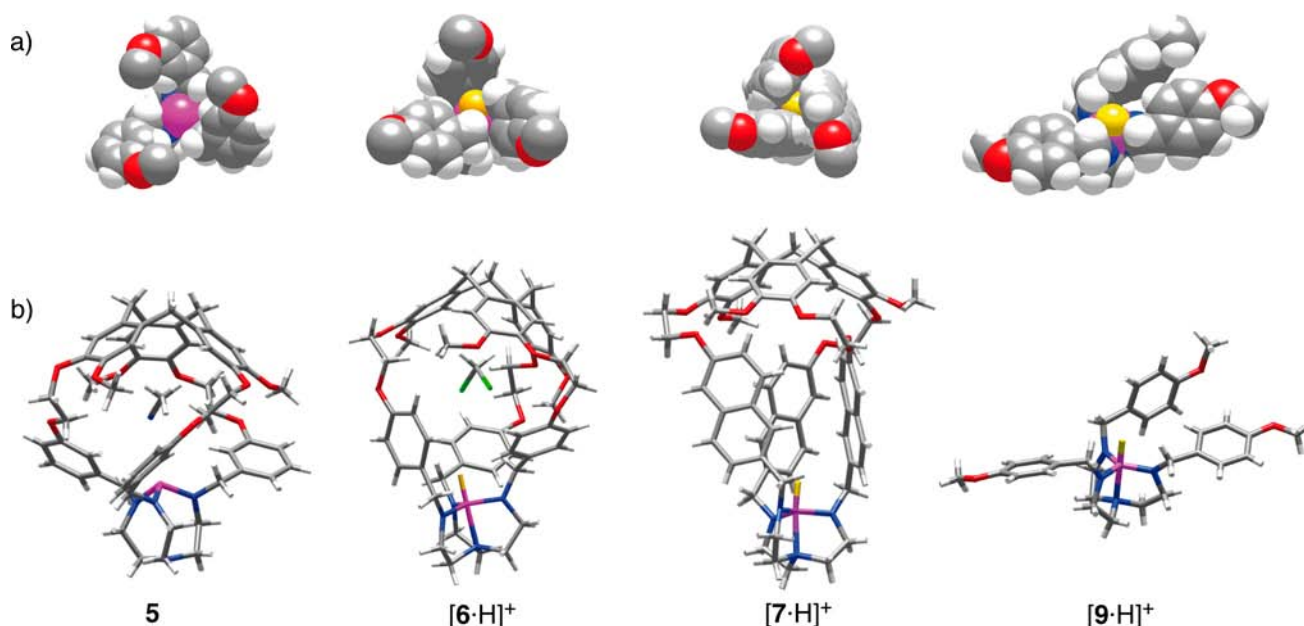


Figure 1. X-ray crystal structures of the encaged Verkade's superbases $\text{CH}_3\text{CN}@5$ and of the azaphosphatranes cations $\text{CH}_2\text{Cl}_2@[\text{6}\cdot\text{H}]^+$, $[\text{7}\cdot\text{H}]^+$, and $[\text{9}\cdot\text{H}]^+$: (a) space filling top views of the phosphorus centers (for 5, $[\text{6}\cdot\text{H}]^+$, and $[\text{7}\cdot\text{H}]^+$ the CTV unit was removed for clarity); (b) stick views (the P–H hydrogen is yellow colored).

Table 1. Selected Geometric Parameters for the Molecular Structures of 5, $[\text{6}\cdot\text{H}]^+\text{Cl}^-$, $[\text{7}\cdot\text{H}]^+\text{Cl}^-$, and $[\text{9}\cdot\text{H}]^+\text{Cl}^-$

parameter	compound			
	5	$[\text{6}\cdot\text{H}]^+\text{Cl}^-$	$[\text{7}\cdot\text{H}]^+\text{Cl}^-$	$[\text{9}\cdot\text{H}]^+\text{Cl}^-$
$d(\text{P}-\text{N}_{\text{eq}})^a$ (Å)	1.694	1.625	1.671	1.664
$d(\text{P}-\text{N}_{\text{ap}})$ (Å)	3.373	1.925	2.005	1.975
$\sum(\text{N}_{\text{eq}}-\text{P}-\text{N}_{\text{eq}})$ (deg)	308.9	358.7	358.2	358.5
$(\text{N}_{\text{eq}}-\text{P}-\text{N}_{\text{ap}})^a$ (deg)		86.2	85.5	85.9
$d(\text{C}_{\text{aro}}\cdots\text{C}_{\text{aro}})^b$ (Å)	5.8	5.1	4.4	6.0
$d(\text{PH}\cdots\text{C}_{\text{aro}})^c$ (Å)		3.0	2.7	3.5
$d(\text{P}\cdots\text{CTV})^d$ (Å)	6.28	8.25	10.21	

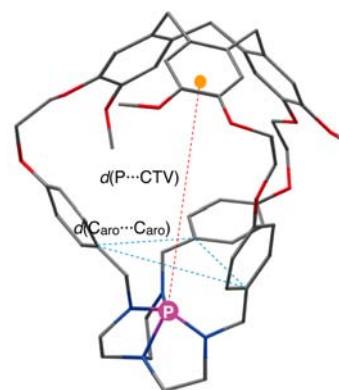
^aAverage of the three values. ^bAverage of the three C...C distances between the $\text{NCH}_2\text{C}_{\text{aro}}$ aromatic carbons. ^cAverage of the three distances between the P–H hydrogen and the $\text{NCH}_2\text{C}_{\text{aro}}$ aromatic carbons. ^dDistance from the barycenter of the CTV aromatic rings to the P atom.

characterized more accurately the accessibility to the hemicyptophane cavity by considering two parameters. First, the three distances $d(\text{C}_{\text{aro}}\cdots\text{C}_{\text{aro}})$ between the first aromatic carbons bound to the NCH_2 groups reflect the opening of the linkers and therefore the access to the phosphorus site.

Second, the distance from the phosphorus atom to the barycenter of the CTV unit, defined from the centroid of the aromatic carbons of the CTV, provides an estimate of the size of the cavity above the phosphatranes core. Both data give a picture of the size of the molecular cavity and of its spatial accessibility (Chart 3).

To discuss the data in Table 1, we will consider the proazaphosphatranes superbases 5 together with the azaphosphatranes $[\text{6}\cdot\text{H}]^+\text{Cl}^-$ and $[\text{7}\cdot\text{H}]^+\text{Cl}^-$. In the three structures, the molecular cavity is well-defined. Going from 5 to $[\text{6}\cdot\text{H}]^+\text{Cl}^-$ and $[\text{7}\cdot\text{H}]^+\text{Cl}^-$, one can see a decrease of the $\text{C}_{\text{aro}}\cdots\text{C}_{\text{aro}}$ distances reflecting the bringing together of the linkers, thus limiting the accessibility to the phosphorus center; the most opened structure is obviously observed with the model $[\text{9}\cdot\text{H}]^+\text{Cl}^-$.

Chart 3



$[\text{6}\cdot\text{H}]^+\text{Cl}^-$. The steric environment in the proximity of the PH^+ cation is also well illustrated through the measure of the $d(\text{PH}\cdots\text{C}_{\text{aro}})$ distance between the PH hydrogen and the $\text{NCH}_2\text{C}_{\text{aro}}$ aromatic carbons of the linkers. From Table 1, the PH hydrogen in $[\text{7}\cdot\text{H}]^+\text{Cl}^-$ is at van der Waals contact distances with the nearest aromatic rings (2.7 Å), which is also evidenced in the molecular structure depicted in Figure 1. In $[\text{6}\cdot\text{H}]^+\text{Cl}^-$ and $[\text{9}\cdot\text{H}]^+\text{Cl}^-$ these distances are respectively 10% and 30% larger than in $[\text{7}\cdot\text{H}]^+\text{Cl}^-$. Concomitantly, there is an increase of the $\text{P}\cdots\text{CTV}$ distance due to the increasing size of the aromatic linkers. Thus, from 5 to $[\text{6}\cdot\text{H}]^+\text{Cl}^-$ and $[\text{7}\cdot\text{H}]^+\text{Cl}^-$ the molecular cavity grows along the pseudo C_3 axis of the molecule but also becomes narrower. The situation for $[\text{7}\cdot\text{H}]^+\text{Cl}^-$ is characteristic of a strong steric hindrance provided by the helical arrangement of the naphthyl groups. Figure 1 shows this trend very well. Accordingly, we observe the encapsulation of a solvent molecule in the molecular cavity of 5 (CH_3CN) and $[\text{6}\cdot\text{H}]^+\text{Cl}^-$ (CH_2Cl_2). In $[\text{7}\cdot\text{H}]^+\text{Cl}^-$ the cavity is too narrow to accommodate a guest molecule.

2.3. pK_a Measurements of the Azaphosphatranes Conjugate Acids. The pK_a values were estimated from

Table 2. pK_a Values of Conjugate Acids of Proazaphosphatrane Bases in Acetonitrile ($T = 298\text{ K}$)^a

parameter	5	8	6	9	7	10
pK_a	31.35	32.90	32.98	32.14	>35	33.17
K_a	4.42×10^{-32}	1.26×10^{-33}	1.03×10^{-33}	7.25×10^{-33}	$<10^{-35}$	6.81×10^{-34}

^aErrors on K_a values are estimated to 10%, giving a maximum error of ± 0.05 on the pK_a values.

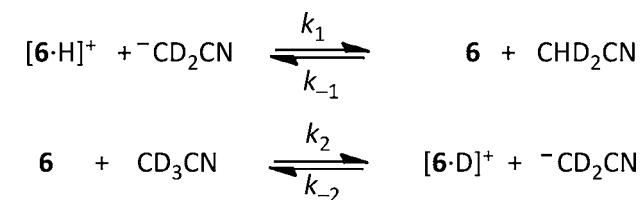
competition experiments: addition of the azaphosphatrane to a solution of the Verkade's superbase **1** ($R = \text{CH}_3$) in CD_3CN led to an equilibrium mixture that was accurately analyzed by ^{31}P and ^1H NMR spectroscopy (see Supporting Information). This afforded reproducible K_a values for the models and the supramolecular compounds (Table 2).²⁶

The encapsulation was found to affect the basicity of the proazaphosphatrane. For example, the encaged superbase **6** is more than 7 times more basic than the model molecule **9** (K_a of 1.03×10^{-33} and 7.25×10^{-33} , respectively), whereas **5** is more than 30 times less basic than its related model compound **8** (K_a of 4.42×10^{-32} and 1.26×10^{-33} , respectively). Interestingly, superbase **7** with naphthyl linkers was found to be much more basic than the model counterpart **10**. Indeed, the encaged species was so basic that we were unable to give an accurate estimation of its pK_a value, since even after several weeks in a sealed NMR tube, no encapsulated superbase **7** could be detected, indicating that the equilibrium is dramatically shifted toward the $[\text{7}\cdot\text{H}]^+\text{Cl}^-$ conjugate acid. As a consequence, the supramolecular superbase is more than 100 times more basic than the model, highlighting how the shape of the inner space of the nanocapsule can modify the thermodynamic parameters of the proton transfer.

These results can be closely related to the geometry of the environment around the phosphorus site. In $[\text{6}\cdot\text{H}]^+\text{Cl}^-$ and $[\text{7}\cdot\text{H}]^+\text{Cl}^-$, the $\text{C}_{\text{aro}}\cdots\text{C}_{\text{aro}}$ or $\text{PH}\cdots\text{C}_{\text{aro}}$ distances, which mainly reflect the closing of the cavity above the phosphorus center, decrease from $[\text{6}\cdot\text{H}]^+\text{Cl}^-$ to $[\text{7}\cdot\text{H}]^+\text{Cl}^-$, providing an enhancement of the cation- π interaction between the acidic proton and the aromatic part of the linkers. Thus, once encapsulated, the acid counterpart of the superbase benefits from this interaction and is much more stabilized in the cage structure than in the model compound. Hence, the congestion of the inner space around the phosphorus center corresponds to an increase of the basicity of the corresponding superbases **6** and **7** when compared to their respective models **9** and **10**. This is particularly obvious for $[\text{7}\cdot\text{H}]^+\text{Cl}^-$, where the proazaphosphatrane form is much more stabilized in the cage structure than in the parent model $[\text{10}\cdot\text{H}]^+\text{Cl}^-$, leading to an improvement of the basicity of the related encaged azaphosphatrane **7** ($pK_a > 35$). In contrast, this additional interaction should be much weaker in $[\text{5}\cdot\text{H}]^+\text{Cl}^-$ because of the longer distances between the aromatic rings and the PH acidic proton. However, in the present case, the model compound **8** is more basic than the hemicyptophane **5**. In the lack of structural data, we assume that the relatively rigid structure of $[\text{5}\cdot\text{H}]^+\text{Cl}^-$, compared to the more flexible structure of the model $[\text{8}\cdot\text{H}]^+\text{Cl}^-$, may favor PH-aromatic interactions in solution for the latter. As a consequence, the supramolecular azaphosphatrane should be less stabilized than its model parent compound, involving a decrease of basicity by encapsulation. Thus, the confinement imposed by a peculiar architecture modifies the space around the reactive site and can create or remove specific interactions, leading to drastic changes in the thermodynamic properties of the azaphosphatrane superbases.

2.4. Kinetic Consequences of the Encapsulation. When $[\text{7}\cdot\text{H}]^+\text{Cl}^-$ was added to a solution of **1** ($R = \text{CH}_3$) in CD_3CN , after more than 5 h no signal characteristic of $[\text{7}\cdot\text{D}]^+\text{Cl}^-$ was observed in the ^{31}P NMR spectrum, whereas when the model compounds were used under the same experimental conditions, the deuterated species appeared immediately. These results showed that the rate for proton transfer dramatically decreased when the phosphorus moiety was located in the inner cavity of the hemicyptophane. Thus, the presence of the cavity affects the rate of this reaction, and an increase of the reaction rate with the size of the cavity is expected, since more space should be available around the phosphorus atom, allowing an easier access to the reactive center. To determine the kinetic parameters, we used the procedure that was described to obtain the rate of proton transfer for **6**.³⁷ The addition of the encaged azaphosphatrane to a solution of **1** ($R = \text{CH}_3$) in CD_3CN allowed a direct monitoring of the kinetics by recording ^{31}P and ^1H NMR spectra as a function of time.

The two acid-base equilibria involved are shown in Scheme 2. Because of the slow rate of proton transfer and the negligible

Scheme 2. Acid-Base Equilibria Involved during the Proton Transfer $[\text{6}\cdot\text{H}]^+ \rightleftharpoons \text{6}$ 

concentration of CHD_2CN compared to those of CD_3CN , only the reaction between the encapsulated azaphosphatrane and $^-\text{CD}_2\text{CN}$ can be considered at short time. This allowed establishing of eqs 1 and 2, where $K_a[\text{6}\cdot\text{H}]^+$, $K_a[\text{1}\cdot\text{H}]^+$, and K_e are respectively the acidity constant of the supramolecular azaphosphatrane, the acidity constant of the Verkade's superbase, and the autoprotolysis constant of acetonitrile, affording the k_1 and k_{-1} values.^{40,41}

$$\frac{d([\text{6}]/[\text{6}\cdot\text{H}]^+)}{dt} = \frac{k_1 k_e}{k_a^{[\text{1}\cdot\text{H}]^+}} \frac{[\text{1}](1 + [\text{6}]/[\text{6}\cdot\text{H}]^+)}{[\text{1}\cdot\text{H}]^+} \quad (1)$$

$$k_{-1} = \frac{K_e}{K_a^{[\text{6}\cdot\text{H}]^+}} k_1 \quad (2)$$

The same equations are applied for each azaphosphatrane \rightleftharpoons proazaphosphatrane acid-base equilibrium studied in this work.

The rate constant for the model molecule **9** has been determined (Table 3) and used as reference. The rate of the proton transfer was found to be much higher with the model molecules than with the encaged superbases, emphasizing the crucial role played by the cavity on the kinetic of proton transfer. Moreover, a strong decrease of the rate constant was observed from **5** to **7**, highlighting how the shape of the space

Table 3. Rate Constants for Proton Transfer in Acetonitrile^a

parameter	5	6	7	9
k_1 (mol L ⁻¹ s ⁻¹)	4.79×10^{-5}	1.88×10^{-6}	1.76×10^{-7}	1.06×10^{-3}
k_{-1} (mol L ⁻¹ s ⁻¹)	6.77×10^{-6}	1.16×10^{-5}	$<1.76 \times 10^{-9}$	0.93×10^{-3}

^aAverage values of at least two experiments, $T = 298$ K.

around the endohedral functionality can affect the kinetics of this reaction.

Examination of the kinetic data in relation with the solid-state structures demonstrates that the more accessible the reactive phosphorus center is ($[9\cdot\text{H}]^+ > 5 > [6\cdot\text{H}]^+ \gg [7\cdot\text{H}]^+$ (it is assumed that the structure of the cavity in 5 and $[5\cdot\text{H}]^+$ is comparable)), the higher the rate of proton transfer is. This explains the extremely low rate of the proton transfer in $[7\cdot\text{H}]^+\text{Cl}^-$ under our experimental conditions. Although we do not have the molecular structure of the superbase 7, the reactive center in 5 is probably more accessible than in 7, accounting for higher rate constant. The decrease of reactivity of the azaphosphatrane superbase toward acetonitrile in the confined space of the hemicyptophane 5 has allowed stabilization of this specific state where superbase and acetonitrile, the two reactive species, are engaged in a same cavity as exemplified by the solid-state structure described above. The location of the acidic and the basic partners, respectively, in the north part and south part of the cavity may explain the decrease of the rate of the proton transfer with hemicyptophane superbases when compared to that of the model molecules. Thus, the $\text{C}_{\text{aro}}\cdots\text{C}_{\text{aro}}$ and $\text{PH}\cdots\text{C}_{\text{aro}}$ distances show that the access to the phosphorus site in 7 and $[7\cdot\text{H}]^+\text{Cl}^-$ is more restricted than in 6 and $[6\cdot\text{H}]^+\text{Cl}^-$ and that 5 and $[5\cdot\text{H}]^+\text{Cl}^-$ present the most opened cage structure, justifying the observed difference in the kinetics of proton transfer.

3. CONCLUSION

In summary, supramolecular proazaphosphatrane superbases presenting various cavity size and shape have been synthesized. It was found that the confinement in these specific architectures affects the $\text{p}K_{\text{a}}$ values: more basic or less basic systems can be obtained, depending on the hemicyptophane structure. Moreover, the encapsulation of the phosphorus moiety strongly affects the rate of proton transfer when compared to that of the model molecules. The rate of proton transfer decreases when the cavity size of the host increases. Accurate inspection of the X-ray molecular structures reveals that the naphthalene linkers block the access to the reactive center. These results indicate the crucial role played by the cavity in the reactivity of active sites encapsulated in a hemicyptophane host. This decrease of reactivity has allowed stabilization of a specific state where the two acido-basic partners are trapped in the confined space of the same nanocapsule. These thermodynamic and kinetic modifications by molecular encapsulation may provide valuable information and better understanding of enzymes or other complex biological systems.

■ ASSOCIATED CONTENT

📄 Supporting Information

Experimental procedures for $\text{p}K_{\text{a}}$ measurements, kinetics experiments, and syntheses and NMR spectra of the new compounds; details for single crystal X-ray analyses of 5 (CCDC-951089), $[7\cdot\text{H}]^+\text{Cl}^-$ (CCDC-951088), and $[9\cdot\text{H}]^+\text{Cl}^-$ (CCDC-951090) in CIF format. This material is available free of charge via the Internet at <http://pubs.acs.org>.

■ AUTHOR INFORMATION

Corresponding Authors

jean-pierre.dutasta@ens-lyon.fr

alexandre.martinez@ens-lyon.fr

Notes

The authors declare no competing financial interest.

■ ACKNOWLEDGMENTS

This work was supported by the French Ministry of Research (Project ANR-2010JCJC 7111 [(Sup)₃Base]).

■ REFERENCES

- (1) Wilcox, J. L.; Bevilacqua, P. C. *J. Am. Chem. Soc.* **2013**, *135*, 7390.
- (2) Rose, I. A. *Brookhaven Symp. Biol.* **1962**, *15*, 293.
- (3) Albery, W. J.; Knowles, J. R. *Biochemistry* **1976**, *15*, 5627.
- (4) Rebek, J., Jr. *Acc. Chem. Res.* **2009**, *42*, 1660.
- (5) Lehn, J.-M. *Rep. Prog. Phys.* **2004**, *67*, 249.
- (6) Yoshizawa, M.; Klosterman, J. K.; Fujita, M. *Angew. Chem., Int. Ed.* **2009**, *48*, 3418.
- (7) Koblenz, T. S.; Wassenaar, J.; Reek, J. N. H. *Chem. Soc. Rev.* **2008**, *37*, 247.
- (8) Feiters, M. C.; Rowan, A. E.; Nolte, R. J. M. *Chem. Soc. Rev.* **2000**, *29*, 375.
- (9) Kirby, A. J. *Angew. Chem., Int. Ed. Engl.* **1996**, *35*, 706.
- (10) Fiedler, D.; Leung, D. H.; Bergman, R. G.; Raymond, K. N. *Acc. Chem. Res.* **2005**, *38*, 349.
- (11) Murakami, Y.; Kikuchi, J.; Hisaeda, Y.; Hayashida, O. *Chem. Rev.* **1996**, *96*, 721.
- (12) Wiester, M. J.; Ulmann, P. A.; Mirkin, C. A. *Angew. Chem., Int. Ed.* **2010**, *50*, 114.
- (13) Adriaenssens, L.; Ballester, P. *Chem. Soc. Rev.* **2013**, *42*, 3261.
- (14) Pluth, M. D.; Bergman, R. G.; Raymond, K. N. *J. Am. Chem. Soc.* **2007**, *129*, 11459.
- (15) Smith, P. B.; Dye, J. L.; Cheney, J.; Lehn, J.-M. *J. Am. Chem. Soc.* **1981**, *103*, 6044.
- (16) Ciampolini, M.; Nardi, N.; Valtancoli, B.; Micheloni, M. *Coord. Chem. Rev.* **1992**, *120*, 223.
- (17) Chambron, J.-C.; Meyer, M. *Chem. Soc. Rev.* **2009**, *38*, 1663.
- (18) Ghosh, I.; Nau, W. M. *Adv. Drug Delivery Rev.* **2012**, *64*, 764.
- (19) Kubik, S. *Top. Curr. Chem.* **2012**, *319*, 1.
- (20) Sather, A. C.; Berryman, O. B.; Moore, C. E.; Rebek, J., Jr. *Chem. Commun.* **2013**, *49*, 6379.
- (21) Harris, K.; Sun, Q.-F.; Sato, S.; Fujita, M. *J. Am. Chem. Soc.* **2013**, *135*, 12497.
- (22) Pollock, J. B.; Cook, T. R.; Stang, P. J. *J. Am. Chem. Soc.* **2012**, *134*, 10607.
- (23) Johnson, A. M.; Moshe, O.; Gamboa, A. S.; Langloss, B. W.; Limtiaco, J. F. K.; Larive, C. K.; Hooley, R. J. *Inorg. Chem.* **2011**, *50*, 9430.
- (24) Young, M. C.; Johnson, A. M.; Gamboa, A. S.; Hooley, R. J. *Chem. Commun.* **2013**, *49*, 1627.
- (25) Lensink, C.; Xi, S. K.; Daniels, L. M.; Verkade, J. G. *J. Am. Chem. Soc.* **1989**, *111*, 3478.
- (26) Kisanga, P. B.; Verkade, J. G.; Schwesinger, R. *J. Org. Chem.* **2000**, *65*, 5431.
- (27) Raders, M. R.; Verkade, J. G. *J. Org. Chem.* **2010**, *75*, 5308.
- (28) Kisanga, P. B.; Verkade, J. G. *Tetrahedron* **2001**, *57*, 467.
- (29) Verkade, J. G.; Kisanga, P. *Tetrahedron* **2003**, *59*, 7819.
- (30) Chintareddy, V. R.; Wadhwa, K.; Verkade, J. G. *J. Org. Chem.* **2009**, *74*, 8118.

- (31) Wadhwa, K.; Chintareddy, V. R.; Verkade, J. G. *J. Org. Chem.* **2009**, *74*, 6681.
- (32) Wadhwa, K.; Verkade, J. G. *J. Org. Chem.* **2009**, *74*, 5683.
- (33) Wadhwa, K.; Verkade, J. G. *J. Org. Chem.* **2009**, *74*, 4368.
- (34) Uргаonkar, S.; Verkade, J. G. *Org. Lett.* **2005**, *7*, 3319.
- (35) Su, W.; McLeod, D.; Verkade, J. G. *J. Org. Chem.* **2003**, *68*, 9499.
- (36) Chintareddy, V. R.; Ellern, A.; Verkade, J. G. *J. Org. Chem.* **2010**, *75*, 7166.
- (37) Dimitrov-Raytchev, P.; Martinez, A.; Gornitzka, H.; Dutasta, J.-P. *J. Am. Chem. Soc.* **2011**, *133*, 2157.
- (38) Chatelet, B.; Payet, E.; Perraud, O.; Dimitrov-Raytchev, P.; Chapellet, L.-L.; Dufaud, V.; Martinez, A.; Dutasta, J.-P. *Org. Lett.* **2011**, *13*, 3706.
- (39) Liu, X.; Ilankumaran, P.; Guzei, I. A.; Verkade, J. G. *J. Org. Chem.* **2000**, *65*, 701.
- (40) Kolthoff, I. M.; Chantooni, M. K., Jr. *J. Phys. Chem.* **1968**, *72*, 2270.
- (41) Rondinini, S.; Longhi, P.; Mussini, P. R.; Mussini, T. *Pure Appl. Chem.* **1987**, *59*, 1693.